

# Spin-density wave in a quantum wire

Oleg A. Starykh

*Department of Physics, University of Utah, Salt Lake City, UT 84112, USA.*

*email: starykh@physics.utah.edu, phone:+1-801-581-6424.*

## Abstract

We present analysis of the interacting quantum wire problem in the presence of magnetic field and spin-orbital interaction. We show that an interesting interplay of Zeeman and spin-orbit terms, facilitated by the electron-electron interaction, results in the spin-density wave (SDW) state when the magnetic field and spin-orbit axes are *orthogonal*. We explore consequences of the spin-orbit interaction for the electron spin resonance (ESR) measurements, and point out that they provide way to probe right- and left-moving excitations of the spin chain separately. We also show that even the problem of two interacting electrons, subjected to the Rashba interaction, is rather non-trivial: In addition to the well-known exchange interaction between electrons' spins, there appears a novel anisotropic spin coupling of van der Waals (non-exchange) origin.

*Keywords:* quantum dots, quantum wires, spin-orbit interaction, renormalization group, bosonization.

*Publication info:* Chapter 30 of *Handbook of Nanophysics: Nanotubes and Nanowires*, edited by Klaus D. Sattler, published by CRC Press (September 2010), ISBN-10: 142007542X.

## Contents

I. Introduction	3
II. Spin-orbit mediated interaction between spins of localized electrons	5
A. Calculation of the vdW coupling	6
B. Effect of magnetic field	9
III. Magnetized quantum wire with spin-orbit interaction	10
A. Non-interacting electrons	10
B. Low-energy description	13
C. Spin-density wave	18
D. Transport properties of the SDW state	21
IV. Conclusions	22
Acknowledgements	24
Appendix A	24
References	31
Figures	35

## I. INTRODUCTION

This paper discusses possibility of realizing spin-density wave (SDW) in a single-channel one-dimensional quantum wire. It should be noted from the outset that purely one-dimensional system of electrons with spin-rotationally invariant interaction between particles (such as the usual Coulomb interaction) cannot have magnetically ordered ground state. At finite temperature any such order is destroyed by thermal fluctuations and the statement is known as the Mermin-Wagner theorem. At zero temperature Goldstone modes associated with spontaneously broken *continuous* spin symmetry destroy the putative order parameter, making the original assumption of the broken symmetry incorrect. Thus SDW states are not possible in one-dimensional wire. (Similarly, one-dimensional superconductivity is not possible as well).

This argument implies that small perturbations that reduce or break the rotational symmetry of the problem acquire very important role. By reducing the symmetry from full spin-rotational invariance ( $SU(2)$ ) to, for example, that of rotations about some particular axis ( $U(1)$ ) or even to a smaller discrete symmetry (such as  $Z_2$ , for example) these symmetry breaking perturbations open up ways to avoid restrictions of the Mermin-Wagner theorem. The crucial role of symmetry in low-dimensional systems can be readily illustrated by differences between the ground states of the  $SU(2)$ -invariant Heisenberg spin chain and the  $Z_2$  invariant Ising one. The former has critical ground state and gapless excitations above it while the latter demonstrates true zero-temperature long-range order with gapful excitations.

In the context of quantum wires and nanostructures in general such a symmetry-lowering perturbation is provided by the ever-present spin-orbital (SO) coupling.

*Spin-orbital interaction* originates from relativistic correction to electron's motion. Textbook example of this consists in considering electron moving with velocity  $\vec{v}$  in external electric field  $\vec{E}_{s-o}$ . In electron's reference frame that field produces magnetic field  $\vec{B}_{s-o} = \vec{E}_{s-o} \times \vec{v}/c^2$ . Then spin-orbital coupling emerges as an interaction of electron's spin  $\vec{S}$  with that magnetic field:

$$H_{s-o} = \frac{g\mu_B}{mc^2} \vec{S} \cdot \vec{E}_{s-o} \times \vec{p} \quad (1)$$

where  $\vec{p} = m\vec{v}$  is the momentum. In atoms  $\vec{E}_{s-o} \propto Ze/r^2$  is the electric field of the nuclei while in fabricated nanostructures  $\vec{E}_{s-o} = -\vec{\nabla}V_{\text{conf}}(r)$  is associated with the structural

asymmetry of the confinement potential. SO coupling due to structure inversion asymmetry (SIA) is known as the Rashba coupling (Bychkov et al. 1984). For the two-dimensional electron gas, where  $\vec{E}_{s-o} \propto \hat{z}\partial_z V_{\text{conf}}(r)$  is related to the normal to the plane of motion gradient of the potential, it reads

$$H_R = \frac{\alpha_R}{\hbar}(\sigma_x p_y - \sigma_y p_x) \quad (2)$$

The Rashba constant  $\alpha_R$  is phenomenological parameter that describes the magnitude of  $\vec{E}_{s-o}$ . The magnitude of asymmetry and hence the Rashba coupling strength can be controlled by the external gate voltage. In addition to the noted asymmetry of confining potentials (which include quantum-well potential that confines electrons to a 2D layer as well as transverse [in-plane] potential that forms the one-dimensional channel (Moroz et al. 1999, 2000a), spin-orbit interaction is inherent to semiconductors of either zinc-blende or wurtzite lattice structures lacking bulk inversion symmetry (Dresselhaus 1955).

Another very interesting system that motivates our investigation is provided by one-dimensional electron surface states on vicinal surface of gold (Mugarza et al. 2002) as well as by electron states of self-assembled gold chains on stepped Si(111) surface of silicon (Crain et al. 2006). In both of the systems one-dimensional ballistic channels appear due to atomic reconstruction of surface layer of atoms, see also (Mugarza et al. 2003, Ortega et al. 2005). The resultant surface electronic states lie within the bandgap of bulk states, and thus, to high accuracy, are decoupled from electrons in the bulk. Spin-orbit interaction is unexpectedly strong in these systems, with the spin-orbit energy splitting of the order of 100 meV. In fact, spin-split subbands of Rashba type have been observed in angular resolved photoemission spectroscopy (ARPES) in both two-dimensional (LaShell et al. 1996) and one-dimensional settings (Mugarza et al. 2002, Crain et al. 2006). The very fact that the two (horizontally) spin-split parabolas are observed in ARPES speaks for high quality and periodicity of the obtained surface channels. As we show below, the most interesting situation involves electrons subjected to both spin-orbital and magnetic fields. While it is perhaps impractical to think of ARPES measurements in the presence of magnetic field, it is quite possible to imagine experiments on *magnetic* metal surfaces (Krupin et al. 2005, Dedkov et al. 2008).

With the current trends in modern state-of-the-art technology, the problem of interacting electrons subject to spin-orbit coupling in one-dimensional conducting channel (be it a

quantum wire or a stepped surface channel) is quite a meaningful one. Recalling that the ordered state in one dimension is only possible when the spin rotational symmetry is sufficiently reduced, it makes sense to also include an external magnetic field, which couples to electron's spin via the standard Zeeman term (Sun et al. 2007, Gangadharaiah et al. 2008a). We shall see below that combined effect of non-commuting spin-orbital and magnetic fields will open up a way to selectively probe left- and right-moving excitations of the quantum wire.

We begin, in Section II, with a “warm-up exercise” of a toy problem of two single-electron quantum dots coupled by strong Coulomb repulsion between electrons and subject to the spin-orbit interaction of Rashba type. The outcome of the simple analysis (Gangadharaiah et al. 2008b), described below, is easy to formulate: even in the absence of exchange interaction between the electrons in different dots, there is an (anisotropic) spin-orbit-mediated coupling between their spins. This coupling comes about from the simple fact that Coulomb interaction correlates *orbital* motion of the electrons. Simply put, the electrons move so as to maximize the distance between them. Since each of the electrons, in turn, has its spin correlated with its orbital motion by the Rashba term, it is perhaps not surprising that the spins of the two electrons end up being correlated as well. What is somewhat surprising is the extreme similarity of this effect with the well-known van der Waals interaction between neutral atoms.

Our main topic - spin-density wave in a quantum wire - is described in Section III. Necessary technical details are outlined in Appendix. Main findings of this work are summarized in Section IV.

## II. SPIN-ORBIT MEDIATED INTERACTION BETWEEN SPINS OF LOCALIZED ELECTRONS

Studies of exchange interaction between localized electrons constitutes one of the oldest topics in quantum mechanics. Strong current interest in the possibility to control and manipulate spin states of quantum dots has placed this topic in the center of spintronics and quantum computation research. As is known from the papers of Dzyaloshinskii (Dzyaloshinskii 1958) and Moriya (Moriya 1960a, 1960b), in the presence of the spin-orbital interaction

(SOI) the exchange is anisotropic in spin space.

Being a manifestation of quantum tunneling, the exchange is exponentially sensitive to the distance between electrons (Bernu et al. 2001). Here we show that when subjected to the spin-orbit interaction, as appropriate for the structure-asymmetric heterostructures and surfaces (Bychkov et al. 1984), interacting electrons acquire a novel *non-exchange* coupling between the spins. The mechanism of this coupling is very similar to that of the well-known van der Waals (vdW) interaction between neutral atoms. This anisotropic interaction is of the *ferromagnetic Ising* type.

### A. Calculation of the vdW coupling.

To illuminate the origin of the vdW coupling, we consider the toy problem of two single-electron quantum dots described by the double well potential (Burkard et al. 1999, Calderon et al. 2006), see Figure 1,

$$\tilde{V}(x_j, y_j) = \frac{m\omega_x^2}{2a^2}(x_j^2 - \frac{a^2}{4})^2 + \frac{m\omega_y^2}{2}y_j^2, \quad (3)$$

where  $\omega_{x/y}$  are confinement frequencies along  $x/y$  directions. The electrons, indexed by  $j = 1, 2$ , are subject to SOI of the Rashba type (Bychkov et al. 1984) with coupling  $\alpha_R$

$$H_{\text{SO}} = \sum_{j=1,2} \alpha_R \vec{p}_j \times \vec{\sigma}_j \cdot \hat{z}, \quad (4)$$

where  $\vec{\sigma}_i$  are the Pauli matrices and  $\hat{z}$  is normal to the plane of motion. Finally, electrons experience mutual Coulomb repulsion so that the total Hamiltonian reads

$$H = \sum_{j=1,2} \left[ \frac{\vec{p}_j^2}{2m} + \tilde{V}(x_j, y_j) \right] + \frac{e^2}{|\vec{r}_1 - \vec{r}_2|} + H_{\text{SO}}. \quad (5)$$

At large separation between the two dots the exchange is exponentially suppressed and the electrons can be treated as distinguishable particles. One then expects that Coulomb-induced correlations in the orbital motion of the electrons in two dots translate, via the spin-orbit interaction, into correlation between their spins. Consider the distance between the dots,  $a$ , much greater than the typical spread of the electron wave functions,  $1/\sqrt{m\omega_x}$ . In this limit the electrons are centered about different wells, and the potential can be approximated as

$$\begin{aligned} V(\vec{r}_1, \vec{r}_2) &\approx \frac{1}{2}m\omega_x^2((x_1 - a/2)^2 + (x_2 + a/2)^2) \\ &+ \frac{1}{2}m\omega_y^2(y_1^2 + y_2^2). \end{aligned} \quad (6)$$

At this stage it is crucial to perform a unitary transformation (Shahbazyan et al. 1994, Aleiner et al. 2001) which removes the linear spin-orbit term from (5)

$$U = \exp[im\alpha_R \hat{z} \cdot (\vec{r}_1 \times \vec{\sigma}_1 + \vec{r}_2 \times \vec{\sigma}_2)]. \quad (7)$$

Owing to the non-commutativity of Pauli spin matrices, SOI can not be eliminated completely, resulting in higher order in the Rashba coupling  $\alpha_R$  contributions as given by  $\tilde{H} = UHU^\dagger$  below

$$\begin{aligned} \tilde{H}_{\text{SO}} = & \sum_{j=1,2} [-m\alpha_R^2 \tilde{L}_j^z \tilde{\sigma}_j^z + \frac{4}{3}m^2\alpha_R^3 (y_j \tilde{\sigma}_j^y + x_j \tilde{\sigma}_j^x) \tilde{L}_j^z \\ & + \frac{2}{3}im^2\alpha_R^3 (y_j \tilde{\sigma}_j^x - x_j \tilde{\sigma}_j^y)] + O(\alpha_R^4). \end{aligned} \quad (8)$$

Here  $\tilde{L}_j^z$  is the angular momentum of the  $j^{\text{th}}$  electron,  $\tilde{L}^z = x\tilde{p}_y - y\tilde{p}_x$ , and *tilde* denotes unitarily rotated operators. The calculation is easiest when the confining energy is much greater than both the Coulomb energy  $e^2/a$  and the spin-orbit energy scale  $\sqrt{m\omega}\alpha_R$ . In terms of the new (primed) coordinates  $\vec{r}'_1 = \vec{r}_1 - \vec{a}/2$  and  $\vec{r}'_2 = \vec{r}_2 + \vec{a}/2$  centered about  $(a/2, 0)$  and  $(-a/2, 0)$ , respectively, the interaction potential  $e^2/|\vec{r}'_1 - \vec{r}'_2 + \vec{a}|$  is expanded in powers of  $1/a$  keeping terms up to second order in the dimensionless relative distance  $(\vec{r}'_1 - \vec{r}'_2)/a$ . The linear term,  $e^2(x'_1 - x'_2)/a^2$ , slightly renormalizes the equilibrium distance between the electrons and can be dropped from further considerations. In terms of symmetric (S) and anti-symmetric (A) coordinates:

$$x_{S/A} = \frac{x'_1 \pm x'_2}{\sqrt{2}}; \quad y_{S/A} = \frac{y'_1 \pm y'_2}{\sqrt{2}}, \quad (9)$$

the quadratic term  $e^2(2(x'_1 - x'_2)^2 - (y'_1 - y'_2)^2)/2a^3$  renormalizes the anti-symmetric frequency  $\omega_{Ax}^2 \rightarrow \omega_x^2 + 4e^2/(ma^3)$  and  $\omega_{Ay}^2 = \omega_y^2 - 2e^2/(ma^3)$  while leaving the symmetric ones unmodified,  $\omega_{Sx}^2 = \omega_x^2$  and  $\omega_{Sy}^2 = \omega_y^2$ . Quite similar to the textbook calculation of the vdW force (Griffiths 2005), the resulting Hamiltonian  $\tilde{H} = \tilde{H}_S + \tilde{H}_A + \tilde{H}_{\text{SO}}$  becomes that of harmonic oscillators

$$\tilde{H}_{S/A} = \frac{\vec{p}_{S/A}^2}{2m} + \frac{m}{2}(\omega_{xS/A}^2 x_{S/A}^2 + \omega_{yS/A}^2 y_{S/A}^2) \quad (10)$$

perturbed by  $\tilde{H}_{\text{SO}} = \tilde{H}_{\text{SO}}^{(2)} + \delta\tilde{H}_{\text{SO}}^{(2)} + \text{O}(\alpha_R^3)$ , where

$$\begin{aligned} \tilde{H}_{\text{SO}}^{(2)} &= -\frac{m\alpha_R^2}{2}[(x_S\tilde{p}_{yS} - y_S\tilde{p}_{xS}) + S \leftrightarrow A](\tilde{\sigma}_1^z + \tilde{\sigma}_2^z) \\ &\quad -\frac{m\alpha_R^2}{2}[(x_S\tilde{p}_{yA} - y_A\tilde{p}_{xS}) + S \leftrightarrow A](\tilde{\sigma}_1^z - \tilde{\sigma}_2^z), \end{aligned} \quad (11)$$

$$\delta\tilde{H}_{\text{SO}}^{(2)} = -\frac{m\alpha_R^2 a}{2\sqrt{2}}[\tilde{p}_{yS}(\tilde{\sigma}_1^z - \tilde{\sigma}_2^z) + \tilde{p}_{yA}(\tilde{\sigma}_1^z + \tilde{\sigma}_2^z)]. \quad (12)$$

It is evident from Eqn. (11,12) that the leading corrections to the ground state energy is obtained either by the excitation of a single  $y$ -oscillator (through (12)) and by the simultaneous excitation of oscillators in both the  $x$  and  $y$  directions (through (11)),

$$\Delta E = -\sum_{i,j=S,A} \frac{|\langle 0|\delta\tilde{H}_{\text{SO}}^{(2)}|1y_i\rangle|^2}{\omega_{iy}} + \frac{|\langle 0|\tilde{H}_{\text{SO}}^{(2)}|1x_i1y_j\rangle|^2}{\omega_{ix} + \omega_{jy}}.$$

It is easy to see that the spin-dependent contributions from  $\delta\tilde{H}_{\text{SO}}^{(2)}$  cancel exactly while those originating from  $\tilde{H}_{\text{SO}}^{(2)}$  do not, resulting in the novel spin interaction

$$\begin{aligned} H_{\text{vdW}} &= \frac{1}{8}m^2\alpha_R^4 \tilde{\sigma}_1^z\tilde{\sigma}_2^z \left( \phi(\omega_{Sy}, \omega_{Sx}) + \phi(\omega_{Ay}, \omega_{Ax}) \right. \\ &\quad \left. - \phi(\omega_{Ay}, \omega_{Sx}) - \phi(\omega_{Sy}, \omega_{Ax}) \right), \end{aligned} \quad (13)$$

where the function  $\phi$  is given by a simple expression

$$\phi(x, y) = \frac{(x - y)^2}{xy(x + y)}. \quad (14)$$

In case of cylindrically symmetric dots,  $\omega_x = \omega_y$ ,

$$H_{\text{vdW}} = -\frac{\alpha_R^4 e^4}{4a^6\omega_x^5} \tilde{\sigma}_1^z\tilde{\sigma}_2^z. \quad (15)$$

The physics of this novel interaction is straightforward: it comes from the interaction-induced correlation of the orbital motion of the two particles, which, in turn, induces correlations between their spins via the spin-orbit coupling. The net Ising interaction would have been zero if not for the shift in frequency of the anti-symmetric mode due to the Coulomb interaction. Note that the coupling strength exhibits the same power-law decay with distance as the standard van der Waals interaction (Griffiths 2005).

From (13), it follows that in the extreme anisotropic limit of  $\omega_y \rightarrow \infty$ , or equivalently, the one-dimensional (1D) limit, there is no coupling between spins. This result is understood by noting that 1D version of SOI, given by  $\alpha_R \sum_j \sigma_j^y p_j^x$ , can be gauged away to all orders in  $\alpha_R$



by a unitary transformation  $U_{1D} = \exp[im\alpha_R(x_1\sigma_1^y + x_2\sigma_2^y)]$ . Hence the absence of the spin-spin coupling in this limit. However, either by including magnetic field (Zeeman interaction, see below) in a direction different from  $\sigma^y$ , or by increasing the dimensionality of the dots by reducing the anisotropy of the confining potential, the spin-orbital Hamiltonian acquires additional non-commuting spin operators. The presence of the mutually non-commuting spin operators (for example,  $\sigma^x$  and  $\sigma^y$  in (4)) makes it impossible to gauge the SOI completely, opening the possibility of fluctuation-generated coupling between distant spins, as in equation (15).

### B. Effect of the magnetic field.

For simplicity, we neglect orbital effects and concentrate on the Zeeman coupling,  $H_Z = -\Delta_z \sum_j \sigma_j^z/2$ , where  $\Delta_z = g\mu_B$ . Unitary transformation (7) changes it to  $H_Z - \Delta_z m\alpha_R a(\sigma_1^x - \sigma_2^x)/2 + \delta\tilde{H}_Z$ . Here

$$\delta\tilde{H}_Z = - \sum_{j=1,2} m\alpha_R \Delta_z (x'_j \tilde{\sigma}_j^x + y'_j \tilde{\sigma}_j^y) \quad (16)$$

describes the coupling between the Zeeman and Rashba terms. In the basis (9) it reduces to

$$\begin{aligned} \delta\tilde{H}_Z = & -m\Delta_z\alpha_R \frac{y_S(\sigma_1^y + \sigma_2^y) + x_S(\sigma_1^x + \sigma_2^x)}{\sqrt{2}}, \\ & -m\Delta_z\alpha_R \frac{y_A(\sigma_1^y - \sigma_2^y) + x_A(\sigma_1^x - \sigma_2^x)}{\sqrt{2}}. \end{aligned} \quad (17)$$

For sufficiently strong magnetic field,  $\Delta_z \gg \sqrt{m\omega}\alpha_R$ ,  $\tilde{H}_{\text{SO}}$  can be neglected in comparison with  $\delta\tilde{H}_Z$ . Calculating second order correction to the ground state energy of the two dots, represented as before by  $\tilde{H}_S + \tilde{H}_A$ , and extracting the spin-dependent contribution, we obtain

$$\Delta E_Z = -\Delta_z^2 \alpha_R^2 \frac{e^2}{a^3} \left( 2 \frac{\sigma_1^x \sigma_2^x}{\omega_x^4} - \frac{\sigma_1^y \sigma_2^y}{\omega_y^4} \right). \quad (18)$$

In the extreme anisotropic limit  $\omega_y \rightarrow \infty$  the dots become 1D and we recover the result of (Flindt et al. 2006). For the isotropic limit  $\omega_x = \omega_y$ , the coupling of spins acquires a magnetic dipolar structure identical to that found in (Trif et al. 2007).

It is interesting to note that for the *in-plane* orientation of the magnetic field,

$$H_Z = \frac{\Delta_z}{2} (\sigma^x \cos \theta + \sigma^y \sin \theta) \quad (19)$$

the unitary transformation leads to

$$U^+ H_Z U = H_Z + \frac{m\alpha_R \Delta_Z}{\sqrt{2}} ((x_S + x_A) \cos \theta + (y_S + y_A) \sin \theta). \quad (20)$$

Calculating again second-order correction to the ground state energy of the two dots to extract the spin-dependent contribution, we obtain an angle-dependent effective Hamiltonian

$$\Delta E_Z = \Delta_Z^2 \alpha_R^2 e^2 \frac{3 \cos^2 \theta - 1}{2a^3} \sigma_1^z \sigma_2^z. \quad (21)$$

Changing direction of the applied field one can change the strength and type of the coupling between spins.

### III. MAGNETIZED QUANTUM WIRE WITH SPIN-ORBIT INTERACTION

#### A. Non-interacting electrons

We next consider significantly more challenging many-body problem of interacting electrons in a quantum wire with Rashba and Zeeman terms. We think of quantum wire as obtained by gating of two-dimensional electron gas. This is modeled by the addition of the transverse confining potential  $V(x) = m\omega^2 x^2/2$  to the non-interacting Hamiltonian  $H_0$  of the system. Then

$$H_0 = \frac{\hbar^2(p_x^2 + p_y^2)}{2m} + V(x) - g\mu_B \frac{\vec{\sigma}}{2} \cdot \vec{B} + H_R, \quad (22)$$

where  $g$  is the effective Bohr magneton,  $B$  is the magnetic field,  $\sigma_\mu$  ( $\mu = x, y, z$ ) are the Pauli matrices and the SO Rashba interaction  $H_R$  is given by (2). When the confining potential is strong enough so that the width of the wire  $\sqrt{\hbar/(2m\omega)}$  is of the order of the electron Fermi-wavelength, only the first sub-band of quantized transverse motion is occupied. The momentum of the transverse standing wave is then replaced by its expectation value,  $p_x \rightarrow \langle p_x \rangle = 0$ . Corrections to this approximation from the omitted term  $\alpha_R \sigma_y p_x$  in (2) produce small spin-dependent variations of the velocities of right- and left-moving particles (Moroz et al. 2000b). Then the Hamiltonian (22) acquires an one-dimensional form

$$H_0 \approx \frac{k^2}{2m} + \alpha_R \sigma_x k - \frac{g\mu_B}{2} \vec{\sigma} \cdot \vec{B}. \quad (23)$$

Here and below  $k$  is electron's momentum along the axis of the wire, which we will denote as  $x$ -axis in the following for notational convenience. We also set  $\hbar = 1$ . Corrections to the

one-dimensional form (23) are controlled by the smallness of the ratios  $\Delta_{s-o}/E_F \ll 1$  and  $\Delta_Z/E_F \ll 1$ , both of which are assumed in this work. Here  $\Delta_{s-o} = \alpha_R k_F$  is the SO splitting,  $\Delta_Z = g\mu_B B$  is the Zeeman splitting, and  $E_F = k_F^2/2m$  is the Fermi-energy which is set by the two-dimensional reservoirs to which the wire is adiabatically connected.

It is easy to see that in the *absence* of magnetic field SOI in (23) can be easily gauged away via the *spin-dependent* shift of the momentum,  $H_0(B=0) \rightarrow (k + m\alpha_R\sigma_x)^2/2m$ . This shift describes the two orthogonal parabolic subbands, which are eigenstates of the matrix  $\sigma_x$  with eigenvalues  $\pm 1/2$ , centered about momenta  $\mp m\alpha_R/2$ . So far, this case does not contain new physics. With Coulomb interaction between electrons included, electrons form Luttinger liquid with somewhat modified critical exponents (Moroz et al. 2000b, Iucci 2003), in comparison with the standard case of no SOI. The reason is that  $H_0(B=0)$  retains the continuous  $U(1)$  symmetry, that of rotations about  $\sigma_x$  axis, which is enough in one dimension for the gapless ground state (Luttinger liquid state) to exist (Giamarchi 2004).

Most interesting situation arises when both SOI and Zeeman terms are present simultaneously and do not commute with each other as happens when spin-orbital axis [ $\sigma_x$  in (23)] is different from the magnetic field direction. Quite generally, we choose magnetic field to be in the  $x-z$  plane, and make an angle  $\pi/2 - \beta$  with the spin-orbital  $x$ -axis. Then  $\vec{B} = B(\sin\beta, 0, \cos\beta)$ . Clearly, for as long as  $\beta < \pi/2$ , the two perturbations, the SO Rashba term and the Zeeman term, do not commute with each other because of the basic property of Pauli matrices  $[\sigma_x, \sigma_z] = -2i\sigma_y \neq 0$ . This implies the loss of the continuous spin-rotational symmetry, and, by our arguments, the possibility of an interesting long-range magnetic order.

The energy eigenvalues of the resulting  $2 \times 2$  matrix, representing Hamiltonian (23), is found as (Levitov et al. 2003, Pereira et al. 2005)

$$\epsilon_{\pm}(k) = \frac{k^2}{2m} \pm \sqrt{(\alpha_R k)^2 + \left(\frac{\Delta_Z}{2}\right)^2 - \Delta_Z \sin\beta \alpha_R k}. \quad (24)$$

Note that the two subbands, corresponding to  $\pm$  signs in (24), are separated by the gap  $\Delta_Z$  at the point  $k = 0$ .

The corresponding eigenstates are easy to find as well. Their most important property consists in the natural fact that they are given by the momentum dependent spinors. For example, for the important case of mutually orthogonal SO and magnetic fields ( $\beta = 0$ ),

they are given by  $|\chi_{\pm}(k)\rangle$ . Here

$$|\chi_{+}(k)\rangle \equiv \begin{bmatrix} \sin \frac{\gamma(k)}{2} \\ \cos \frac{\gamma(k)}{2} \end{bmatrix}, |\chi_{-}(k)\rangle \equiv \begin{bmatrix} \cos \frac{\gamma(k)}{2} \\ -\sin \frac{\gamma(k)}{2} \end{bmatrix}, \quad (25)$$

and we introduced rotation angle  $\gamma(k)$

$$\gamma(k) = \arctan \frac{2\alpha_R k}{\Delta_z}. \quad (26)$$

Observe that spin directions in each subband vary with the momentum. This, of course, is direct consequence of the “momentum-dependent magnetic field” produced by the SO interaction  $H_R$ .

The obtained ( $\pm$ ) subbands are filled up to the Fermi energy  $E_F = k_F^2/2m$ , which is parameterized by the Fermi-momentum  $k_F$  defined in the absence of both SO and magnetic field terms in (23). The Fermi-momenta  $k_{\pm}^{R/L}$  of the subbands are easily found from (24). Note that for  $\beta \neq 0$  the Fermi-points are not symmetric about the origin, i.e.  $k_{\pm}^R \neq -k_{\pm}^L$ . Of crucial importance for the following is the observation that single-particle states at the Fermi-points of the two subbands have finite overlap. That is,  $\langle \chi_{+}(k_{+}^{R/L}) | \chi_{-}(k_{-}^{R/L}) \rangle \neq 0$  as long as  $\Delta_{s-o} \neq 0$ . (They are, of course, always orthogonal at the same momentum:  $\langle \chi_{+}(k) | \chi_{-}(k) \rangle = 0$ .)

This fact allows for a qualitative discussion of the *inter-subband interaction* effects in  $|\chi_{\pm}\rangle$  basis. Namely, the finite overlap between single-particle states of ( $\pm$ ) bands guaranties that Coulomb interaction will open up *pair-tunneling processes* when a pair of electrons from the opposite Fermi-points of the one subband (say,  $k_{+}^R$  and  $k_{+}^L$ ) tunnels into a similar pair of states in the other subband (at  $k_{-}^R$  and  $k_{-}^L$ ). Such a process clearly conserves energy (both initial and final states are at  $E_F$ ). For the case of orthogonal SO and magnetic field axes ( $\beta = 0$  above) such a two-particle process also conserves momentum. This is because for  $\beta = 0$  (and only in this case) the initial and final momenta of the pair are equal, and are simply zero ( $k_{+}^R + k_{+}^L = k_{-}^R + k_{-}^L = 0$ ), see Figure 2. The only exception to this is provided by the limit  $\Delta_{s-o} = 0$ , when  $\gamma = 0$ , see (26). In this limit spinors  $|\chi_{\pm}\rangle$  become standard momentum-independent eigenstates of the Zeeman term,  $|\chi_{\pm}\rangle \rightarrow |\downarrow\rangle, |\uparrow\rangle$ . Such Zeeman-split subbands are clearly orthogonal,  $\langle \downarrow | \uparrow \rangle = 0$ , and do not allow for the pair with, say,  $S^z = -1$ , to hop into the up-spin subband, and vice versa. Such a tunneling requires “conversion” of

$S^z = -1$  pair into that with  $S^z = +1$  and is only possible when  $S^z$  is not a good quantum number, i.e. it requires spin non-conservation. This is exactly what the SO interaction does – it breaks the  $U(1)$  symmetry about the axis of the field. Thus, as long as  $\gamma(k_F) \neq 0$ , the inter-subband pair-tunneling is possible. In view of the similarity with superconducting pair scattering, the inter-subband pair-tunneling process is often called Cooper scattering (Starykh et al. 2000). Its existence represents qualitative difference between the wires with and without the spin-orbital terms. Quantitative consequences of the Cooper scattering are analyzed in details in the next Section.

Observe that non-orthogonal orientation,  $\beta > 0$ , results in momentum mismatch between the pairs in the two subbands, see Figure 3. This mismatch suppresses inter-subband pair-tunneling, see (50) and discussion after it.

## B. Low-energy description

We now focus on the quantitative description of the problem. This is done by linearizing the *unperturbed* Hamiltonian (the one with  $\alpha_R = 0$  and  $B = 0$ ) in terms of low-energy fermions  $R_s$  ( $L_s$ ) that live near  $+k_F$  ( $-k_F$ ) Fermi-points. In terms of these, kinetic energy is simply

$$H_{\text{kin}} = \sum_{s=\uparrow,\downarrow} \int dx \{-iv_F R_s^+ \partial_x R_s + iv_F L_s^+ \partial_x L_s\} \quad (27)$$

where  $v_F = k_F/m$  is the Fermi-velocity and  $s$  is the spin index. It is crucial at this stage to write the kinetic energy as a sum of commuting *charge* and *spin* parts (Sugawara formulation),  $H_{\text{kin}} = H_{\text{charge}}^0 + H_{\text{spin}}^0$ , where

$$H_{\text{charge}}^0 = \frac{\pi v_F}{2} \int dx \{J_R J_R + J_L J_L\}, \quad (28)$$

$$H_{\text{spin}}^0 = \frac{2\pi v_F}{3} \sum_{a=x,y,z} \int dx \{J_R^a J_R^a + J_L^a J_L^a\}, \quad (29)$$

and we introduced *charge*

$$J_R = \sum_s R_s^+ R_s, \quad J_L = \sum_s L_s^+ L_s, \quad (30)$$

and *spin* currents ( $a = x, y, z$ )

$$J_R^a = \sum_{s,s'} R_s^+ \frac{\sigma_{ss'}^a}{2} R_{s'}, \quad J_L^a = \sum_{s,s'} L_s^+ \frac{\sigma_{ss'}^a}{2} L_{s'}. \quad (31)$$

Magnetic field comes in via the Zeeman term

$$H_Z = -\Delta_z \int dx \{ \cos \beta (J_R^z + J_L^z) + \sin \beta (J_R^x + J_L^x) \} \quad (32)$$

while the Rashba SO interaction reads

$$H_R = 2\Delta_{s-o} \int dx \{ J_R^x - J_L^x \}. \quad (33)$$

Note that both perturbations are written in terms of chiral (right and left) spin currents only. The relative minus sign between the right and left spin currents in  $H_R$  follows from oddness of the Rashba term under spatial inversion ( $x \rightarrow -x$ ) which interchanges right and left moving excitations. The coupling to magnetic field  $H_Z$  of course is not sensitive to this operation.

The full non-interacting Hamiltonian (23) is given by the sum of the terms above,  $H_0 = H_{\text{kin}} + H_Z + H_R$ . The usefulness of the introduced spin-current formulation follows from the fact that it makes it explicitly clear that the two perturbations couple only to the spin sector of the theory.

This observation greatly simplifies subsequent calculations. We first notice that it is now easy to include *interactions* in the description. The interaction term can also be written as the sum of charge and spin contributions. Moreover, despite the fact one-dimensional electrons interact with each other strongly (being constrained to a line, they simply can not avoid collisions with each other), the interaction correction to the spin sector is small,

$$H_{\text{bs}} = -g \int dx \vec{J}_R \cdot \vec{J}_L. \quad (34)$$

This interaction term is known as the *backscattering* correction, its amplitude is determined by the  $2k_F$ -component of the interaction potential:  $g \sim U(2k_F) > 0$ . For comparison, the interaction correction to the charge sector is controlled by the zero-momentum component of the potential, which is always much greater than the backscattering one,  $U(0) \gg U(2k_F)$ .

The backscattering interaction correction is not only numerically small, it is *marginally irrelevant* in the renormalization group sense (to be clarified below). This means that the coupling constant  $g$  is in fact a function of energy (and/or momentum), which diminishes in magnitude as the energy approaches zero. This irrelevance implies that to the zeroth approximation  $H_{\text{bs}}$  can be often (but not always, see below!) omitted altogether. When

appropriate, such an approximation implies an *extended* symmetry of  $H_{\text{spin}}^0$ : being a sum of right and left spin current contributions,  $H_{\text{spin}}^0$  is invariant under *independent* rotations of right and left spin currents.

Our solution of the problem exploits this extended symmetry. First we observe that perturbations  $H_Z$  and  $H_R$  add up to a single “vectorial” term

$$V = \int dx \{d_R J_R^x - d_L J_L^x - d_z (J_R^z + J_L^z)\}, \quad (35)$$

where  $d_R = 2\Delta_{s-o} - \sin[\beta]\Delta_z$ ,  $d_L = 2\Delta_{s-o} + \sin[\beta]\Delta_z$ , and  $d_z = \cos[\beta]\Delta_z$ . Extended symmetry of  $H_{\text{spin}}^0$  allows us to immediately conclude that right and left spin currents experience different total magnetic fields. The right spin current  $\vec{J}_R$  couples to  $\vec{h}_R$  with magnitude  $h_R = \sqrt{d_R^2 + d_z^2}$  while the left current  $\vec{J}_L$  experiences  $\vec{h}_L$  of magnitude  $h_L = \sqrt{d_L^2 + d_z^2}$ . The two fields are different unless  $\beta = 0$  when  $h_R = h_L$ .

Formal way to see this (Schnyder et al. 2008) is provided by rotation of the right (left) spin current  $\vec{J}_R$  ( $\vec{J}_L$ ) by angle  $\theta_R$  ( $\theta_L$ ) about the  $\hat{y}$ -axis,

$$\vec{J}_R = \mathcal{R}(\theta_R)\vec{M}_R, \quad \vec{J}_L = \mathcal{R}(\theta_L)\vec{M}_L, \quad (36)$$

where  $\mathcal{R}$  is the rotation matrix

$$\mathcal{R}(\theta) = \begin{pmatrix} \cos[\theta] & 0 & -\sin[\theta] \\ 0 & 1 & 0 \\ \sin[\theta] & 0 & \cos[\theta] \end{pmatrix}. \quad (37)$$

The rotation angles are given by  $\tan[\theta_R] = d_R/d_z$  and  $\tan[\theta_L] = -d_L/d_z$ . These chiral rotations transform  $V$  into

$$V = - \int dx \{h_R M_R^z + h_L M_L^z\}. \quad (38)$$

It is worth pointing again that  $H_{\text{kin}}^0$  is invariant under the rotations and is given by a simple substitution  $\vec{J} \rightarrow \vec{M}$  in (29),

$$H_{\text{spin}}^0 = \frac{2\pi v_F}{3} \sum_{a=x,y,z} \int dx \{M_R^a M_R^a + M_L^a M_L^a\}. \quad (39)$$

Implications of Eq.(38) are quite unusual: by varying the direction of the magnetic field one can selectively couple to right- and left-moving spin excitations. In particular, by lining  $\vec{B}$

along the spin-orbital axis, which happens for  $\beta = \pi/2$ , one can adjust the magnitude  $|\vec{B}|$  so that, for example,  $h_R = 0$  while  $h_L \neq 0$ . It turns out that electron-spin-resonance (ESR) can in effect measure these chiral effective magnetic fields. More precisely, one finds that intensity  $I_{\text{esr}}$  of the ESR signal in general is given by a sum of two terms, representing two independent chiral contributions from (38). Specifically, for a generic  $h_R \neq h_L$  situation one should observe two sharp lines (De Martino et al. 2002, De Martino et al. 2004, Gangadharaiah et al. 2008a)

$$I_{\text{esr}}(\omega) = (\cos^2 \theta_R + 1)h_R\delta(\omega - |h_R|) + (\cos^2 \theta_L + 1)h_L\delta(\omega - |h_L|). \quad (40)$$

While certainly interesting, this result is based on complete neglect of the residual interaction between spin excitations  $H_{\text{bs}}$ . Little thinking shows that in this approximation equations (38) and (39) in fact represent a system of non-interacting fermions,  $R'_s$  and  $L'_s$ , which are rotated version of  $R_s, L_s$  pair in (27). The relation between ‘old’ and ‘new’ fermions is simple

$$R_s = e^{i\theta_R\sigma_y/2}R'_s, \quad L_s = e^{i\theta_L\sigma_y/2}L'_s \quad (41)$$

where  $\theta_{R/L}$  are the rotation angles from (36). That is, new (primed) fermions parameterize vector field  $\vec{M}_{R/L}$  in the same way as the old (unprimed) ones parameterize fields  $\vec{J}_{R/L}$ . For example, under the right rotation  $\mathcal{R}(\theta_R)$

$$\vec{J}_R = \sum_{s,s'} R_s^+ \frac{\vec{\sigma}_{ss'}}{2} R_{s'} \rightarrow \vec{M}_R = \sum_{s,s'} R'_s{}^+ \frac{\vec{\sigma}_{ss'}}{2} R'_{s'}. \quad (42)$$

Using this relation one can un-do steps that led us from (27) to (28) and (29) (naturally, scalar charge fluctuations are not affected by the rotation at all) and find that (39) and (28) simply add up to a kinetic energy term (27) expressed via primed fermions  $R'_s, L'_s$ . The extended symmetry discussed above is then simply reflection of the symmetry of (27) which, for example, is invariant under independent rotations of right- and left-movers.

It must be also clear now that, irrespective of the basis used, non-interacting fermions can not describe ordered state of any kind. This simple fact forces us to consider the fate of the two-particle backscattering interaction in greater detail. Under the rotations discussed



$H_{\text{bs}}$  changes to

$$\begin{aligned}
H_{\text{bs}} &= -g \int dx \vec{M}_R \mathcal{R}^T(\theta_R) \mathcal{R}(\theta_L) \vec{M}_L = \\
&= -g \int dx \{ \cos[\chi] (M_R^x M_L^x + M_R^z M_L^z) \\
&\quad + \sin[\chi] (M_R^x M_L^z - M_R^z M_L^x) + M_R^y M_L^y \},
\end{aligned} \tag{43}$$

where  $\chi = \theta_R - \theta_L$  is the *relative* rotation angle.

Despite complicated appearance, (43) can be dealt with rather easily (Gangadharaiah et al. 2008a, Schnyder et al. 2008). The key to the subsequent progress is provided by switching to *abelian* bosonization technique, which is well suited for analyzing systems with  $U(1)$  symmetry. Within this powerful technique kinetic energy (39) turns into energy of free conjugated pair of bosons,  $\varphi$  and  $\theta$ ,

$$H_{\text{spin}}^0 = \frac{v_F}{2} \int dx \{ (\partial_x \varphi)^2 + (\partial_x \theta)^2 \}. \tag{44}$$

At the same time  $V$  transforms into linear in bosons form

$$V = - \int dx \left( \frac{v_F t_\varphi}{\sqrt{2\pi}} \partial_x \varphi_\sigma + \frac{v_F t_\theta}{\sqrt{2\pi}} \partial_x \theta_\sigma \right), \tag{45}$$

where

$$t_\varphi = (h_L + h_R)/2v_F, \quad t_\theta = (h_L - h_R)/2v_F. \tag{46}$$

Observe that now  $V$  can be absorbed in  $H_{\text{spin}}^0$  with the help of simple shift of bosonic fields

$$\begin{aligned}
\varphi_\sigma &\rightarrow \varphi_\sigma + \frac{t_\varphi x}{\sqrt{2\pi}}, \\
\theta_\sigma &\rightarrow \theta_\sigma + \frac{t_\theta x}{\sqrt{2\pi}}.
\end{aligned} \tag{47}$$

The shift comes at a price – transverse components  $M_{R/L}^{x,y}$  acquire oscillating position-dependent factors

$$M_R^+ \rightarrow M_R^+ e^{-i(t_\varphi - t_\theta)x}, \quad M_L^+ \rightarrow M_L^+ e^{i(t_\varphi + t_\theta)x}. \tag{48}$$

The major consequence of this is that every term in  $H_{\text{bs}}$ , with a single exception of  $M_R^z M_L^z$ ,

acquires an oscillating pre-factor

$$\begin{aligned}
H_{\text{bs}} = & -g \int dx \left( \cos[\chi] M_R^z M_L^z + \right. \\
& + \frac{\cos[\chi] - 1}{4} (M_R^+ M_L^+ e^{i2t_\theta x} + \text{h.c.}) \\
& + \frac{\cos[\chi] + 1}{4} (M_R^+ M_L^- e^{-i2t_\varphi x} + \text{h.c.}) \\
& \left. + \frac{\sin[\chi]}{2} (M_L^z M_R^+ e^{-i(t_\varphi - t_\theta)x} - M_R^z M_L^+ e^{i(t_\varphi + t_\theta)x} + \text{h.c.}) \right).
\end{aligned} \tag{49}$$

The oscillating terms, which represent momentum-non-conserving two-particle scattering processes, average out to zero. This results in drastic simplification of the backscattering interaction,  $H'_{\text{bs}} = -g \cos[\chi] \int dx M_R^z M_L^z$ , which holds for as long as  $t_\varphi \neq t_\theta \neq 0$ . Using again bosonization rules, we see that the final Hamiltonian,  $H_{\text{spin}}^0 + H'_{\text{bs}}$ , retains its harmonic form

$$H_{\text{spin}}^0 + H'_{\text{bs}} = \frac{v_F}{2} \int dx \left\{ \frac{1}{K} (\partial_x \varphi_\sigma)^2 + K (\partial_x \theta_\sigma)^2 \right\}, \tag{50}$$

where the dimensionless interaction parameter  $K = 1 + g \cos[\chi]/(4\pi v_F) > 1$  is introduced. This Hamiltonian allows one to calculate any spin correlation function of interest, provided that one remains within the low-energy approximation assumed in the derivation. Such a situation corresponds to  $\beta > 0$  and is illustrated in Fig. 3: inter-subband pair tunneling is suppressed by the finite momentum mismatch.

### C. Spin-density wave

We will not follow this well-understood route and instead focus on the case of  $t_\theta = 0$ , which is realized for  $\beta = 0$ . In this case  $\chi = 2\theta_R = -2\theta_L$ . This special arrangement corresponds to the case of mutually orthogonal directions of the spin-orbital and magnetic fields, when the electron subbands are centered about  $k = 0$  momentum. This is the configuration when inter-subband pair-tunneling is allowed by momentum conservation, see Figure 2. Focusing again on the non-oscillating terms only, we observe that interaction between spin fluctuations is described by

$$\begin{aligned}
H_{\text{bs}}^\perp = & -g \int dx \left\{ \cos[\chi] M_R^z M_L^z + \right. \\
& \left. + \frac{\cos[\chi] - 1}{4} (M_R^+ M_L^+ + M_R^- M_L^-) \right\}.
\end{aligned} \tag{51}$$

Unlike the previously discussed  $H'_{\text{bs}}$ , the interaction term  $H_{\text{bs}}^\perp$  does not reduce to simple quadratic form of  $\varphi$  and  $\theta$  fields. In fact it represents non-trivial interacting problem analysis of which requires renormalization group (RG) treatment. Omitting technical details which can be found in modern textbooks (Giamarchi 2004, Gogolin, Nersesyan and Tsvelik 1999) (brief review is given in Appendix , see also (Giamarchi et al. 1988)), we cite the result

$$\frac{dg_z}{d\ell} = \frac{g_\perp^2}{2\pi v_F}, \quad \frac{dg_\perp}{d\ell} = \frac{g_\perp g_z}{2\pi v_F} \quad (52)$$

where  $g_z$  (correspondingly,  $g_\perp/2$ ) is the coefficient of  $M_R^z M_L^z$  (correspondingly,  $M_R^+ M_L^+$ ) term in  $H_{\text{bs}}^\perp$ . Here dimensionless RG parameter  $\ell = \ln(a'/a)$  represents effect of integrating out fluctuations on the length scales between  $a'$  and  $a$ . The system of two coupled RG equations is nothing but famous Berezinskii-Kosterlitz-Thouless (BKT) renormalization group (Giamarchi 2004, Gogolin, Nersesyan and Tsvelik 1999), flow diagram of which is shown in Figure 4. Its solution depends on the initial values of the couplings involved,  $g_z(0) = g \cos[\chi]$  and  $g_\perp(0) = g(\cos[\chi] - 1)/2$ , and is conveniently parameterized by the integral of motion  $Y(\chi) = g_\perp^2 - g_z^2$ . It turns out that the solution is towards *strong coupling* (meaning that  $|g_{z,\perp}(\ell)| \rightarrow \infty$  for sufficiently large  $\ell$ ) for all possible angles  $\chi \in (0, \pi)$ . This diverging solution imply instability towards a correlated spin state with finite energy gap between the ground and excited states. That gap can be estimated as  $\Delta \sim v_F e^{-\ell_0}$  where  $\ell_0$  is the RG scale on which the couplings diverge. (The derivation of RG equations is perturbative in nature and relies on the smallness of the ratio  $g_{z,\perp}/v_F$ . Thus solution with  $g_{z,\perp}/v_F \geq 1$  can not, strictly speaking, be trusted. But taking  $\ell_0$  for an *estimate* above remains sensible.) The *minimal* value of  $\ell_0$  occurs for  $Y = 0$  (this corresponds to a line separating regions I and II in Figure 4), when  $\chi_0 = 2 \arccos[\sqrt{2/3}]$ . The system then simplifies to a single equation,

$$\frac{dg_z}{d\ell} = \frac{g_z^2}{2\pi v_F}, \quad (53)$$

solution of which is:  $g_z(\ell) = g_z(0)/(1 - g_z(0)\ell/(2\pi v_F))$ . Thus  $\ell_0 = 2\pi v_F/g_z(0) = 3(2\pi v_F/g)$ . The corresponding gap is exponentially small,  $\Delta/v_F \sim \exp[-6\pi v_F/g] \ll 1$ .

We now consider the physical meaning of the Cooper instability. This is best done by noting that the abelian form of the term that drives the instability,  $(M_R^+ M_L^+ + \text{h.c.})$ , is just  $\cos \sqrt{8\pi} \theta_\sigma$ . More specifically, abelian bosonization of (51) results in

$$H_{\text{bs}}^\perp = \int dx \left\{ -\frac{g_z}{8\pi} [(\partial_x \varphi_\sigma)^2 - (\partial_x \theta_\sigma)^2] + \frac{g_\perp}{4\pi^2 a_0^2} \cos[\sqrt{8\pi} \theta_\sigma] \right\}. \quad (54)$$

As the coupling  $g_{\perp}$  of that terms grows large (and positive) under the renormalization, the energy is minimized when  $\theta_{\sigma}$  is at one of the semi-classical minima  $\theta_{\sigma}^{\text{cl}} = (m + \frac{1}{2})\sqrt{\pi/2}$  ( $m$  is integer). The energy cost of massive fluctuations  $\delta\theta_{\sigma}$  near these minima represents the spin gap estimated above.

Physical meaning of these minima follows from the analysis of spin correlation functions. We consider spin density  $S^a = \Psi_s^{\dagger} \sigma_{s,s'}^a \Psi_{s'}/2$ , which is defined with respect to the standard spin basis,  $s = \uparrow, \downarrow$ . Consider first  $2k_F$ -components of the spin density. We find (Gangadharaiah et al. 2008a) (see Appendix, note that we use gauge where  $\eta_{\uparrow}\eta_{\downarrow} = i$ )

$$\begin{aligned}
& \begin{pmatrix} S^x \\ S^y \\ S^z \end{pmatrix}_{2k_F} = -\frac{\cos[\sqrt{2\pi}\varphi_{\rho} + 2k_F x]}{\pi a_0} \times \\
& \times \begin{pmatrix} -\sin[\sqrt{2\pi}\theta_{\sigma}] \\ \cos[\frac{\chi}{2}] \cos[\sqrt{2\pi}\theta_{\sigma}] + \sin[\frac{\chi}{2}] \cos[\sqrt{2\pi}\varphi_{\sigma} + t_{\varphi} x] \\ \sin[\sqrt{2\pi}\varphi_{\sigma}] \end{pmatrix} \\
& \rightarrow -\frac{\cos[\sqrt{2\pi}\varphi_{\rho} + 2k_F x]}{\pi a_0} \begin{pmatrix} \pm 1 \\ 0 \\ 0 \end{pmatrix}. \tag{55}
\end{aligned}$$

The last line of the above equation is somewhat symbolic, with zeros representing *exponentially* decaying correlations of the corresponding spin components,  $S^{y,z}$ . Here  $\hat{z}$ -component is disordered by strong quantum fluctuations of  $\varphi_{\sigma}$  field, which is *dual* to the ordered  $\theta_{\sigma}$  one. The  $\hat{y}$ -component is absent because  $\cos[\sqrt{2\pi}\theta_{\sigma}^{\text{cl}}] = 0$ . Thus Cooper order found here in fact represents spin-density-wave (SDW) order at momentum  $2k_F$  of the  $\hat{x}$ -component of spin density, as discussed previously in (Sun et al. 2007). Note that the ordered component,  $S^x$ , is oriented along the spin-orbital axis  $\sigma^x$ . Observe also that  $S^x$  ordering is of *quasi-LRO* type as it involves free charge boson,  $\varphi_{\rho}$ . As a result, spin correlations do decay with time and distance, but very slowly  $\langle S^x(x)S^x(0) \rangle \sim \cos[2k_F x] x^{-K_{\rho}}$ . The rate of the spatial decay is determined by the interactions in the charge sector only, via the parameter  $K_{\rho}$ .

The result (55) also hints a possibility of truly long-range-ordered spin correlations in the insulating state of the wire – Heisenberg spin chain. There the charge field  $\varphi_{\rho}$  is absent, which can be mimicked by setting  $K_{\rho} \rightarrow 0$  in the spin correlation function above. Then

$\langle S^x(x)S^x(0) \rangle \sim \cos[2k_F x] = (-1)^x$ , describes long-range ordered SDW state of the magnetic insulator (Gangadharaiah et al. 2008a) (with asymmetric Dzyaloshinskii-Moriya interaction in place of the Rashba coupling considered here).

#### D. Transport properties of the SDW state

SDW<sub>x</sub> state manifests itself not only in spin correlations. It turns out that its response to a weak potential scattering (impurity) is rather non-trivial. We consider here a weak delta-function impurity  $V(x) = V_0\delta(x)$ , with strength  $V_0$ , located at the origin. The condition  $V_0 \ll \Delta$  means that impurity can be considered as a weak perturbation to the established SDW phase. (The limit of strong impurity,  $V_0 \gg \Delta$ , is rather standard: impurity destroys the SDW and the wire flows into an insulator at low energies (Kane et al. 1992).)

The interaction of electrons with an impurity potential  $V(x)$  is given by

$$\hat{V} = \int dx V(x) \sum_{s=\uparrow,\downarrow} \Psi_s^\dagger(x)\Psi_s(x). \quad (56)$$

As usual, it is the *backscattering* ( $\rho_{2k_F}$ ) part of the charge density that has to be considered, since it describes the process in which an electron with momentum  $+k_F$  scatters back into  $-k_F$  state losing thereby large momentum  $2k_F$ :  $\rho_{2k_F}(x=0) = \sum_s (R_s^\dagger L_s + \text{h.c.})$ . Performing the rotation and bosonizing we find, see Appendix and (A33) in particular,

$$\rho_{2k_F}(x=0) = \frac{-2 \sin[\sqrt{2\pi}\varphi_\rho]}{\pi a_0} \left( \cos\left[\frac{\chi}{2}\right] \cos[\sqrt{2\pi}\varphi_\sigma] + \sin\left[\frac{\chi}{2}\right] \cos[\sqrt{2\pi}\theta_\sigma] \right). \quad (57)$$

We now observe that setting  $\theta_\sigma \rightarrow \theta_\sigma^{\text{cl}} = (m + \frac{1}{2})\sqrt{\pi/2}$ , as appropriate for the SDW phase, *nullifies* the backscattering component of the density (57). The first term gets killed by diverging fluctuations of  $\varphi_\sigma$ , *dual* to  $\theta_\sigma$ . Intriguingly, the second contribution is also zero because  $\cos[\sqrt{2\pi}\theta_\sigma^{\text{cl}}] = \pm \cos[\pi/2] = 0$ .

Physical explanation of this unusual result is grounded in the observation that  $x$ -components of electron's spins at  $\pm k_F$  points are *anti-parallel*, see (55). At the same time, scattering off potential impurity does not affect the spin of the scattered electron. Hence electron with, say, spin along  $+\hat{x}$  axis and momentum  $+k_F$  is scattered to a state with momentum  $-k_F$  and the same spin orientation. However the Fermi-point only supports states with spin along  $-\hat{x}$ , see Figure 1, for as long as one is interested in low-energy states

(energy well below  $\Delta$ ). Thus, at such low energies there is no electron backscattering and potential impurity does not affect electron's propagation along the wire (Sun et al. 2007, Gangadharaiah et al. 2008a).

The situation is similar to that in recently proposed edge states in quantum spin Hall system (Kane et al. 2005). There, gapless spin-up and spin-down excitations propagate in opposite directions along the edge, which forbids single-particle backscattering. Interacting electrons, however, can backscatter off the impurity in pairs (Xu et al. 2006, Wu et al. 2006).

Pairwise scattering of electrons off the weak impurity can be analyzed as follows (Starykh et al. 2000, Orignac et al. 1997, Egger et al. 1998). We parametrize  $\theta_\sigma = \theta_\sigma^{\text{cl}} + \delta\theta$  and expand the relevant cosine term in Hamiltonian (54) to second order in fluctuations  $\delta\theta$ . One obtains a *massive* term  $\propto \Delta(\delta\theta)^2$  in the Hamiltonian, which causes exponential decay in correlation functions of the dual  $\varphi_\sigma$  field. In particular,  $\langle \cos \sqrt{2\pi}\varphi_\sigma(0, \tau) \cos \sqrt{2\pi}\varphi_\sigma(0, \tau') \rangle$  will decay as  $\exp[-\Delta|\tau - \tau'|]$ . Substituting  $\theta_\sigma = \theta_\sigma^{\text{cl}} + \delta\theta$  in the second term in (57) converts it into  $\sin[\chi/2] \sin[\sqrt{2\pi}\varphi_\rho] \sin[\sqrt{2\pi}\delta\theta]$ . Correlations of  $\sin[\sqrt{2\pi}\delta\theta]$  are also short-ranged

$$\langle \sin[\sqrt{2\pi}\delta\theta(\tau)] \sin[\sqrt{2\pi}\delta\theta(\tau')] \rangle \approx \frac{\Delta_c}{v_F k_F} \sinh[K_0(\Delta|\tau - \tau'|)], \quad (58)$$

where  $K_0(x) \sim e^{-x}/\sqrt{x}$  (for  $x \gg 1$ ) is the modified Bessel function (see (Starykh et al. 2000)). The two exponentially decaying contributions add up (in second order perturbation theory in impurity strength  $V_0$ ) to produce an effective two-particle backscattering potential  $\propto (V_0^2/\Delta) \cos[\sqrt{8\pi}\varphi_\rho(0, \tau)]$ . This term describes interaction-generated *two-particle* backscattering. However, it is relevant only for strongly repulsive interactions, when  $K_\rho < 1/2$ . We are thus left with *irrelevant* impurity potential for both single- and two-particle scattering events. Hence, we conclude that as long as approximation  $V_0 \ll \Delta$  is justified and for not too strong repulsion, when  $1/2 \leq K_\rho \leq 1$ , the SDW state is not sensitive to weak disorder.

This unusual prediction should manifest itself in strong sensitivity of the conductance of the quantum wire to the direction of the applied magnetic field. Weak potential impurity will remain irrelevant (and, thus, not observable) for as long as applied magnetic field is directed perpendicular to the spin-orbital ( $\sigma^x$  here) axis. By either turning the magnetic field off, or simply rotating the sample (so that angle  $\beta$  between the magnetic field and the spin-orbital axis changes from 0), one should observe that conductance of the wire deteriorates. With  $\beta \neq 0$  the wire will eventually turn insulating in the zero-temperature limit.

## IV. CONCLUSIONS

Spin-orbital interactions result in reduction of spin-rotational symmetry from  $SU(2)$  to  $U(1)$  in one-dimensional quantum wires and spin chains. This reduction, however, is not sufficient to change the critical (Luttinger liquid) nature of the one-dimensional interacting fermions. The situation changes dramatically once external magnetic field is applied. Most interesting situation occurs when the applied field is oriented along the axis orthogonal to the spin-orbital axis of the wire. The resulting combination of two non-commuting perturbations, taken together with electron-electron interactions, leads to a novel spin-density-wave order in the direction of the spin-orbital axis.

The physics of this order is elegantly described in terms of spin-non-conserving (Cooper) pair tunneling processes between Zeeman-split electron subbands. The tunneling matrix element is finite only due to the presence of the spin-orbit interaction, which allows for spin-up to spin-down (and vice versa) conversion.

The resulting SDW state affects both spin and charge properties of the wire. In particular, it suppresses effect of (weak) potential impurity, resulting in the interesting phenomena of negative magnetoresistance in one-dimensional setting.

Even when the magnetic field and spin-orbital directions are not orthogonal, an arrangement when the critical Luttinger state survives down to the lowest temperature, the problem remains interesting. In this geometry an ESR experiment should reveal two separate lines, which represent separate responses of right- and left-moving spin fluctuations in the system.

It is worth pointing out that unusual consequences of the interplay of spin-orbit and electron interactions are not restricted to one-dimensional systems only. As shown in Section II, Coulomb-coupled two-dimensional quantum dots acquire a novel van der Waals-like anisotropic interaction between spins of the localized electrons. The strength of this Ising interaction is determined by the forth power of the Rashba coupling  $\alpha_R$ .

We hope that our work will stimulate experimental search and studies of strongly interacting quasi-one-dimensional systems with sizable spin-orbital interaction, in particular regarding their response to the (both magnitude and direction) applied magnetic field and/or magnetization. ESR studies of quantum wires and spin chain materials are very desirable as well.

## ACKNOWLEDGMENTS

I would like to thank my collaborators on this project, Jianmin Sun and Suhas Gangadharaiah, for their invaluable contributions to this topic. I also thank Suhas Gangadharaiah for careful reading of the manuscript. I am deeply grateful to Andreas Schnyder and Leon Balents for the collaboration on quantum kagomé antiferromagnet where the trick of chiral rotations of spin currents has originated. I would like to thank I. Affleck, T. Giamarchi, K. Matveev, E. Mishchenko, M. Oshikawa, M. Raikh, and Y.-S. Wu for discussions and suggestions at various stages of this work. I thank Petroleum Research Fund of the American Chemical Society for the financial support of this research under the grant PRF 43219-AC10.

## Appendix A: Bosonization basics

Bosonization starts by expressing the fermionic operators  $\Psi_s(x)$

$$\Psi_s = R_s e^{ik_F x} + L_s e^{-ik_F x}. \quad (\text{A1})$$

in terms of right ( $R_s$ ) and left ( $L_s$ ) movers of unperturbed single-channel quantum wire. These represent electrons with momenta near the right,  $+k_F$ , and the left,  $-k_F$ , Fermi momenta of the wire. They are then represented via exponentials of the chiral bosonic  $\phi_{R/L,s}$  fields (Gogolin, Nersisyan and Tselik 1999, Giamarchi 2004, Lin et al. 1997) as follows

$$R_s = \frac{\eta_s}{\sqrt{2\pi a_0}} e^{i\sqrt{4\pi}\phi_{R,s}}, \quad L_s = \frac{\eta_s}{\sqrt{2\pi a_0}} e^{-i\sqrt{4\pi}\phi_{L,s}}, \quad (\text{A2})$$

where  $a_0 \sim k_F^{-1}$  is the short distance cutoff and  $\eta_s$  are the Klein factors which are introduced to ensure the correct anti-commutation relations for the fermions with different spin projection  $s = \uparrow = +1$  and  $s = \downarrow = -1$ . The bosonic operators obey the following commutation relations:

$$[\phi_{R,s}, \phi_{L,s'}] = \frac{i}{4} \delta_{ss'}; \quad (\text{A3})$$

$$[\phi_{R/L,s}(x), \phi_{R/L,s'}(y)] = \pm \frac{i}{4} \delta_{ss'} \text{sign}(x - y), \quad (\text{A4})$$

the first of which, (A3), ensures anticommutation between right and left movers from the same subband, while the second is needed for the anticommutation between like species (i.e.



right with right, left with left). Klein factors anticommute

$$\{\eta_s, \eta_{s'}\} = 2\delta_{ss'}, \quad \eta_s^\dagger = \eta_s. \quad (\text{A5})$$

In the following we choose the gauge where  $\eta_{+1}\eta_{-1} = i$ . The chiral  $\phi_{R/L,s}$  are expressed in terms of  $\phi_s$  and its dual  $\theta_s$  as follows

$$\phi_{R,s} = \frac{\phi_s - \theta_s}{2}; \quad \phi_{L,s} = \frac{\phi_s + \theta_s}{2}, \quad (\text{A6})$$

The bosonized form of the Hamiltonian is obtained by making use of equations (A2) through (A6), as well as the following results for (chiral) densities

$$\begin{aligned} R_s^\dagger R_s &= \frac{\partial_x \phi_{R,s}}{\sqrt{\pi}} = \frac{\partial_x(\phi_s - \theta_s)}{\sqrt{4\pi}}, \\ L_s^\dagger L_s &= \frac{\partial_x \phi_{L,s}}{\sqrt{\pi}} = \frac{\partial_x(\phi_s + \theta_s)}{\sqrt{4\pi}} \end{aligned} \quad (\text{A7})$$

It then follows from the above formalism that kinetic energy of fermions with *linear* dispersion, see (27), transforms into kinetic energy of bosons

$$H_{\text{kin}} = \frac{v_F}{2} \sum_s \int dx \{(\partial_x \phi_s)^2 + (\partial_x \theta_s)^2\}. \quad (\text{A8})$$

Next we introduce *charge* and *spin* bosons via

$$\varphi_\rho = \frac{1}{\sqrt{2}}(\phi_\uparrow + \phi_\downarrow), \quad \varphi_\sigma = \frac{1}{\sqrt{2}}(\phi_\uparrow - \phi_\downarrow), \quad (\text{A9})$$

and similar for the  $\theta_{\rho,\sigma}$ . These independent modes allow us to represent kinetic Hamiltonian as a sum of two commuting, charge-only and spin-only, parts

$$H_{\text{kin}} = H_{\text{kin},\rho} + H_{\text{kin},\sigma} = \frac{v_F}{2} \sum_{\nu=\rho,\sigma} \int dx \{(\partial_x \phi_\nu)^2 + (\partial_x \theta_\nu)^2\}. \quad (\text{A10})$$

The utility of this representation consists in the observation that *interaction* between electrons separates into charge and spin contributions as well. Interaction between electrons is described by

$$H_{\text{int}} = \frac{1}{2} \sum_{s,s'} \int dx dx' U(x-x') \Psi_s^+(x) \Psi_{s'}^+(x') \Psi_{s'}(x') \Psi_s(x), \quad (\text{A11})$$

where  $U(x)$  is just (screened by gates) Coulomb interaction. Using (A1) we observe that

$$\Psi_s^+(x) \Psi_s(x) = R_s^+ R_s + L_s^+ L_s + e^{-i2k_F x} R_s^+ L_s + e^{i2k_F x} L_s^+ R_s. \quad (\text{A12})$$

Focusing on momentum-conserving terms and using identity (see (30),(31))

$$\sum_{s,s'} R_s^+ R_{s'} L_{s'}^+ L_s = 2\vec{J}_R \cdot \vec{J}_L + \frac{1}{2} J_R J_L, \quad (\text{A13})$$

we express  $H_{\text{int}} = H_{\text{int},\rho} + H_{\text{int},\sigma}$  as a sum of charge and spin contributions

$$H_{\text{int},\rho} = \int dx \left\{ \frac{1}{2} U(0) (J_R^2 + J_L^2) + (U(0) - \frac{1}{2} U(2k_F)) J_R J_L \right\}, \quad (\text{A14})$$

$$H_{\text{int},\sigma} = \int dx \left\{ -2U(2k_F) \vec{J}_R \cdot \vec{J}_L \right\}. \quad (\text{A15})$$

The interaction is parameterized by two constants,  $U(0)$  and  $U(2k_F)$ , which are zeroth and  $2k_F$  components of the Fourier transform of  $U(x - x')$ :  $U(q) = \int dx U(x) e^{iqx}$ . Clearly  $U(0) \gg U(2k_F)$  for a smoothly decaying potential. Observe that the spin sector involves only the weakest of the two interaction constants. This term, (A15), is the backscattering correction (34) described in the main text.

The total charge Hamiltonian can be conveniently written in a quadratic boson form

$$H_\rho = \frac{v_\rho}{2} \int dx \left\{ K_\rho^{-1} (\partial_x \varphi_\rho)^2 + K_\rho (\partial_x \theta_\rho)^2 \right\} \quad (\text{A16})$$

with charge velocity  $v_\rho = v_F(1 + U(0)/(\pi v_F)) > v_F$  and dimensionless interaction parameter  $K_\rho = 1 - (2U(0) - U(2k_F))/(2\pi v_F) < 1$ . This important result is the starting point for many interesting features of strongly correlated one-dimensional electrons, as it allows for an essentially exact calculation of the low-energy properties of these electrons in terms of free bosons  $\varphi_\rho$  and  $\theta_\rho$ .

The spin Hamiltonian does not have simple harmonic appearance because the product of spin currents in (A15) includes very non-linear  $\cos[\sqrt{8\pi}\varphi_\sigma]$  term. Nevertheless the progress is possible by attacking (A15) using perturbative (in small  $U(2k_F)/v_F$  ratio) RG, as described in the main text. The key idea is to exploit the charge-spin separation to the fullest: by its very derivation the spin backscattering correction (A15) involves only spin modes  $\varphi_\sigma$  and  $\theta_\sigma$ . It is then allowed to disregard the charge part,  $H_{\text{int},\rho}$ , altogether and treat  $H_{\text{int},\sigma}$  as the only perturbation to the free Hamiltonian (27). The charge part of kinetic energy  $H_{\text{kin},\rho}$ , which is contained in (27), is guaranteed (by the independence of charge and spin bosons) not to affect the result of such calculation in any way. The end result is that one can formulate perturbation theory in question in terms of weakly interacting fermions again! The bosonization is used here only to make the phenomenon of the charge-spin separation

explicit on the level of operators. This observation provides for a convenient short-cut in deriving the operator-product relations between spin currents which are required for the perturbative RG (see (Starykh et al. 2005) for more details).

In general, one is interested in RG equation for the anisotropic current-current interaction term,

$$H'_\sigma = - \sum_{a=x,y,z} \int dx \{g_a J_R^a J_L^a\}. \quad (\text{A17})$$

For example, in (51) we have  $g_z = g \cos[\chi]$ ,  $g_x = -g_y = g(\cos[\chi] - 1)$  and  $g = 2U(2k_F)$ . We expand partition function  $Z = \int e^S$ , where the action  $S = S_0 - \int d\tau H'_\sigma$ , in powers of the perturbation  $H'_\sigma$ . The unperturbed action  $S_0$  describes free spin excitations which, by the logic outlined above, are faithfully represented by the free Hamiltonian (27). To second order in  $g$  one has

$$\begin{aligned} Z = \int e^{S_0} \{ & 1 + \sum_{a=x,y,z} \int dx d\tau g_a J_R^a(x, \tau) J_L^a(x, \tau) \\ & + \frac{1}{2} \sum_{a,b} g_a g_b \int dx d\tau dx' d\tau' J_R^a(x, \tau) J_R^b(x', \tau') J_L^a(x, \tau) J_L^b(x', \tau') + \dots \} \quad (\text{A18}) \end{aligned}$$

Renormalization is possible because the last term in the brackets contains terms which reduce to the second term, i.e. to  $H'_\sigma$ . This follows from the non-trivial property of the product of spin currents

$$J_R^a(x, \tau) J_R^b(x', \tau') = \frac{\delta^{ab}}{8\pi^2(v_F\tau - ix)^2} + \frac{i\epsilon^{abc} J_R^c(x, \tau)}{2\pi(v_F\tau - ix)} + \text{less singular terms}. \quad (\text{A19})$$

This result follows from applying Wick's theorem (justified here because the unperturbed Hamiltonian is just  $H_{\text{kin}}$ ) and making all possible fermion pairings. These are constrained by the fact that the only non-zero correlations are between like fermions (right with right, and left with left) of the same spin, as dictated by the structure of (27). Thus the singular denominator in the equation above is just the Green's function of right fermions. Another ingredient of (A19) is the well-known Pauli matrix property:

$$\sigma^a \sigma^b = \delta^{ab} + i \sum_c \epsilon^{abc} \sigma^c. \quad (\text{A20})$$

The product of left currents has similar expansion with the obvious replacement  $v_F\tau - ix \rightarrow v_F\tau + ix$ , as appropriate for the left-moving particles. With the help of these operator-product

expansions, the last term (denoted  $V$  here) simplifies to

$$V = \text{const} - \frac{1}{2} \sum_{a,b,c,d} g_a g_b \int dx d\tau dx' d\tau' \frac{\epsilon^{abc} \epsilon^{abd} J_R^c(x, \tau) J_L^d(x, \tau)}{4\pi^2 (v_F \tau - ix)(v_F \tau + ix)}, \quad (\text{A21})$$

where the constant is the contribution from the first term in (A19). Switching to the center-of-mass and relative coordinates we finally have

$$V = \frac{1}{2} \sum_c \delta g_c \int dx d\tau J_R^c(x, \tau) J_L^c(x, \tau) \quad (\text{A22})$$

where

$$\delta g_c = -\frac{1}{2} \sum_{a,b \neq c} \frac{g_a g_b}{2\pi v_F} \int_a^{a'} \frac{dr}{r} = -\frac{1}{2} \sum_{a,b \neq c} \frac{g^a g^b}{2\pi v_F} \ln\left(\frac{a'}{a}\right) \quad (\text{A23})$$

is given by the integral over relative coordinate. In terms of RG scale  $\ell = \ln(a'/a)$  the differential change in the coupling  $g_c$  follows

$$\frac{dg_c}{d\ell} = - \sum_{a,b \neq c} \frac{g_a g_b}{4\pi v_F}. \quad (\text{A24})$$

This, of course, contains three equations

$$\begin{aligned} \frac{dg_x}{d\ell} &= -\frac{g_y g_z}{2\pi v_F}, \\ \frac{dg_y}{d\ell} &= -\frac{g_x g_z}{2\pi v_F}, \\ \frac{dg_z}{d\ell} &= -\frac{g_x g_y}{2\pi v_F}. \end{aligned} \quad (\text{A25})$$

RG equations in the main text follows from the ones above by simple re-arrangements.

To obtain bosonic representation of spin in (55), one needs to start with the definition of  $2k_F$  component of spin density,

$$\vec{S}_{2k_F}(x) = \frac{1}{2} \sum_{s,s'} R_s^+ \vec{\sigma}_{s,s'} L_{s'} e^{-i2k_F x} + L_s^+ \vec{\sigma}_{s,s'} R_{s'} e^{i2k_F x} \quad (\text{A26})$$

Next we need to account for the rotation (41). This leads us to consider the following objects

$$e^{-i\theta_R \sigma_y / 2} \sigma_x e^{i\theta_L \sigma_y / 2} = e^{-i(\theta_R + \theta_L) \sigma_y / 2} \sigma_x = \sigma_x, \quad (\text{A27})$$

where we made use of (A20) and the fact that in the current geometry  $\theta_R = -\theta_L$ . Hence we find that  $S^x$  and  $S^z$  components of the spin density are not affected by the rotation while  $S^y$  component does change. Indeed,

$$e^{-i\theta_R \sigma_y / 2} \sigma_y e^{i\theta_L \sigma_y / 2} = e^{-i(\theta_R - \theta_L) \sigma_y / 2} \sigma_y = e^{-i\chi \sigma_y / 2} \sigma_y. \quad (\text{A28})$$

Hence

$$S_{2k_F}^y = \cos\left[\frac{\chi}{2}\right] \frac{1}{2} \sum_{s,s'} \{R_s'^+ \sigma_{s,s'}^y L_{s'}' e^{-i2k_F x} + \text{h.c.}\} + \sin\left[\frac{\chi}{2}\right] \frac{1}{2} \sum_{s,s'} \{iR_s'^+ L_{s'}' e^{-i2k_F x} + \text{h.c.}\} \quad (\text{A29})$$

We now bosonize primed fermions using (A2), (A3), (A6) and (A9) as well as the Baker-Hausdorff formulae

$$e^A e^B = e^B e^A e^{[A,B]}, \quad e^A e^B = e^{A+B} e^{[A,B]/2}. \quad (\text{A30})$$

In this way we obtain

$$S_{2k_F}^y = \frac{1}{\pi a_0} \cos[\sqrt{2\pi}\varphi_\rho + 2k_F x] (\cos\left[\frac{\chi}{2}\right] \cos[\sqrt{2\pi}\theta_\sigma] + \sin\left[\frac{\chi}{2}\right] \cos[\sqrt{2\pi}\varphi_\sigma + t_\varphi x]). \quad (\text{A31})$$

The appearance of the position-dependent phase  $t_\varphi x$  in the last term in the brackets is due to the shift (47), where we need to use  $t_\varphi = h_R/v_F = \sqrt{4\Delta_{s-o}^2 + \Delta_z^2}/v_F$  in order to account for the mutually orthogonal orientation of the spin-orbital and magnetic field axes. The other, unrotated, components of the spin density vector are obtained by similar calculations, resulting in (55) of the main text.

Calculation of the backscattering ( $2k_F$ ) component of the density  $\rho_{2k_F}$  proceeds very similarly,

$$\begin{aligned} \rho_{2k_F} &= \sum_s R_s^+ L_s e^{-i2k_F x} + L_s^+ R_s e^{i2k_F x} \rightarrow \cos\left[\frac{\chi}{2}\right] \sum_s \{R_s'^+ L_s' e^{-i2k_F x} + \text{h.c.}\} + \\ &+ \sin\left[\frac{\chi}{2}\right] \sum_{s,s'} \{-iR_s'^+ \sigma_{s,s'}^y L_s' e^{-i2k_F x} + \text{h.c.}\} \end{aligned} \quad (\text{A32})$$

Subsequent bosonization leads to

$$\rho_{2k_F} = -\frac{2}{\pi a_0} \sin[\sqrt{2\pi}\varphi_\rho + 2k_F x] (\cos\left[\frac{\chi}{2}\right] \cos[\sqrt{2\pi}\varphi_\sigma + t_\varphi x] + \sin\left[\frac{\chi}{2}\right] \cos[\sqrt{2\pi}\theta_\sigma]). \quad (\text{A33})$$

Bosonized form of the nonlinear Cooper term  $M_R^+ M_L^+$  follows from

$$\begin{aligned} M_R^+ &= \frac{1}{2} \sum_{s,s'} R_s'^+ (\sigma_x + i\sigma_y)_{s,s'} R_{s'}' = \frac{i}{4\pi a_0} e^{-i\sqrt{2\pi}(\varphi_\sigma - \theta_\sigma)}, \\ M_L^+ &= \frac{1}{2} \sum_{s,s'} L_s'^+ (\sigma_x + i\sigma_y)_{s,s'} L_{s'}' = \frac{i}{4\pi a_0} e^{i\sqrt{2\pi}(\varphi_\sigma + \theta_\sigma)}. \end{aligned} \quad (\text{A34})$$

This result, together with (A4), implies that  $M_R^+ M_L^+ + \text{h.c.} \sim \cos[\sqrt{8\pi}\theta_\sigma]$ . Note also that equations (A34) explain the effect of the shift (47) on transverse components  $M_{R/L}^\pm$  of the magnetization, equation (48).

## References

- Aleiner, I.L. and V.I. Fal'ko, 2001. Spin-Orbit Coupling Effects on Quantum Transport in Lateral Semiconductor Dots. *Phys. Rev. Lett.* **87**: 256801.
- Bernu, B., L. Candido, and D.M. Ceperley, 2001. Exchange Frequencies in the 2D Wigner Crystal. *Phys. Rev. Lett.* **86**: 870.
- Bychkov, Yu.A. and E.I. Rashba, 1984. Oscillatory effects and the magnetic susceptibility of carriers in inversion layers. *J. Phys. C* **17**: 6039.
- Burkard, G., D. Loss, and D.P. DiVincenzo, 1999. Coupled quantum dots as quantum gates. *Phys. Rev. B* **59**: 2070.
- Calderon, M.J., B. Koiller, and S. Das Sarma, 2006. Exchange coupling in semiconductor nanostructures: Validity and limitations of the Heitler-London approach. *Phys. Rev. B* **74**: 045310.
- Crain, J.N. and F.J. Himpsel, 2006. Low-dimensional electronic states at silicon surfaces. *Appl. Phys. A* **82**, 431.
- Dedkov, Yu. S. , M. Fonin, U. Rüdiger, and C. Laubschat, 2008. Rashba Effect in the Graphene/Ni(111) System. *Phys. Rev. Lett.* **100**: 107602.
- De Martino, A., R. Egger, K. Hallberg, and C.A. Balseiro, 2002. Spin-Orbit Coupling and Electron Spin Resonance Theory for Carbon Nanotubes. *Phys. Rev. Lett.* **88**: 206402.
- De Martino, A., R. Egger, F. Murphy-Armando, and K. Hallberg, 2004. Spin-orbit coupling and electron spin resonance for interacting electrons in carbon nanotubes. *J. Phys.: Condens. Matter* **16**: S1437.
- Dresselhaus, G. 1955. Spin-Orbit Coupling Effects in Zinc Blende Structures. *Phys. Rev.* **100**: 580.
- Dzyaloshinskii, I.E. 1958. A thermodynamic theory of weak ferromagnetism of antiferromagnetics. *J. Phys. Chem. Solids* **4**: 241-255.
- Egger, R. and A.O. Gogolin, 1998. Correlated transport and non-Fermi liquid behavior in single-wall carbon nanotubes. *Eur. Phys. J. B* **3**: 281-300.
- Flindt, C., A.S. Sorensen, and K. Flensberg, 2006. Spin-Orbit Mediated Control of Spin Qubits. *Phys. Rev. Lett.* **97**: 240501.
- Gangadharaiah, S., J. Sun, and O.A. Starykh, 2008a. Spin-orbital effects in magnetized quantum wires and spin chains. *Phys. Rev. B* **78**: 054436.

Gangadharaiah, S., J. Sun, and O.A. Starykh, 2008b. Spin-Orbit-Mediated Anisotropic Spin Interaction in Interacting Electron Systems. *Phys. Rev. Lett.* **100**: 156402.

Gogolin, A.O., A.A. Nersesyan, and A.M. Tsvelik, 1999. *Bosonization and strongly correlated systems*. Cambridge: Cambridge University Press.

Griffiths, D.J. 2005. *Introduction to Quantum Mechanics*. Upper Saddle River: Pearson, 2nd ed. p. 286.

Giamarchi, T. and H. J. Schulz, 1988. Theory of spin-anisotropic electron-electron interactions in quasi-one-dimensional metals. *Journal de Physique* **49**: 819-835.

Giamarchi, T. 2004. *Quantum physics in one dimension*. Oxford: Oxford University Press.

Iucci, A. 2003. Correlation functions for one-dimensional interacting fermions with spin-orbit coupling. *Phys. Rev. B* **68**: 075107.

Kane, C.L. and M.P.A. Fisher, 1992. Transmission through barriers and resonant tunneling in an interacting one-dimensional electron gas. *Phys. Rev. B* **46**: 15233.

Kane, C.L. and E.J. Mele, 2005. Quantum Spin Hall Effect in Graphene. *Phys. Rev. Lett.* **95**: 226801.

Krupin, O., G. Bihlmayer, K. Starke, et al. 2005. Rashba effect at magnetic metal surfaces. *Phys. Rev. B* **71**: 201403.

LaShell, S., B.A. McDougall, and E. Jensen, 1996. Spin Splitting of an Au(111) Surface State Band Observed with Angle Resolved Photoelectron Spectroscopy. *Phys. Rev. Lett.* **77**: 3419.

Levitov, L.S. and E.I. Rashba, 2003. Dynamical spin-electric coupling in a quantum dot. *Phys. Rev. B* **67**: 115324.

Lin, H.-H., L. Balents, and M.P.A. Fisher, 1997. N-chain Hubbard model in weak coupling. *Phys. Rev. B* **56**: 6569-6593.

Moriya, T. 1960a. New Mechanism of Anisotropic Superexchange Interaction. *Phys. Rev. Lett.* **4**: 228-230.

Moriya, T. 1960b. Anisotropic Superexchange Interaction and Weak Ferromagnetism. *Phys. Rev.* **120**: 91-98.

Moroz, A.V. and C.H.W. Barnes, 1999. Effect of the spin-orbit interaction on the band structure and conductance of quasi-one-dimensional systems. *Phys. Rev. B* **60**: 14272-14285.

- Moroz, A.V. and C.H.W. Barnes, 2000a. Spin-orbit interaction as a source of spectral and transport properties in quasi-one-dimensional systems. *Phys. Rev. B* **61**: R2464-R2467.
- Moroz, A.V., K.V. Samokhin and C.H.W. Barnes, 2000b. Theory of quasi-one-dimensional electron liquids with spin-orbit coupling. *Phys. Rev. B* **62**: 16900-16911.
- Mugarza, A., A. Mascaraque, V. Repain, et al. 2002. Lateral quantum wells at vicinal Au(111) studied with angle-resolved photoemission. *Phys. Rev. B* **66**: 245419.
- Mugarza, A. and J.E. Ortega, 2003. Electronic states at vicinal surfaces. *J. Phys.: Condens. Matter* **15**: S3281-S3310.
- Orignac, E. and T. Giamarchi, 1997. Effects of disorder on two strongly correlated coupled chains. *Phys. Rev. B* **56**: 7167-7188.
- Ortega, J.E., M. Ruiz-Osés, J. Gordón, et al. 2005. One-dimensional versus two-dimensional electronic states in vicinal surfaces. *New J. Phys.* **7**: 101.
- Pereira, R.G. and E. Miranda, 2005. Magnetically controlled impurities in quantum wires with strong Rashba coupling. *Phys. Rev. B* **71**: 085318.
- Schnyder, A.P., O.A. Starykh, and L. Balents, 2008. Spatially anisotropic Heisenberg kagome antiferromagnet. *Phys. Rev. B* **78**: 174420.
- Shahbazyan, T.V. and M.E. Raikh, 1994. Low-Field Anomaly in 2D Hopping Magnetoresistance Caused by Spin-Orbit Term in the Energy Spectrum. *Phys. Rev. Lett.* **73**: 1408-1411.
- Starykh, O.A., D.L. Maslov, W. Häusler, and L.I. Glazman, 2000. Gapped Phases of Quantum Wires. In *Low-dimensional systems: interactions and transport properties*, ed. T. Brandes, 37-78. *Lecture Notes in Physics* **544**. Berlin: Springer.
- Starykh, O.A., A. Furusaki, and L. Balents, 2005. Anisotropic pyrochlores and the global phase diagram of the checkerboard antiferromagnet. *Phys. Rev. B* **72**: 094416.
- Sun, J., S. Gangadharaiah, and O.A. Starykh, 2007. Spin-Orbit-Induced Spin-Density Wave in a Quantum Wire. *Phys. Rev. Lett.* **98**: 126408.
- Trif, M., V.N. Golovach, and D. Loss, 2007. Spin-spin coupling in electrostatically coupled quantum dots. *Phys. Rev. B* **75**: 085307.
- Wu, C., B.A. Bernevig, and S.-C. Zhang, 2006. Helical Liquid and the Edge of Quantum Spin Hall Systems. *Phys. Rev. Lett.* **96**: 106401.
- Xu, C. and J.E. Moore, 2006. Stability of the quantum spin Hall effect: Effects of



interactions, disorder, and  $Z_2$  topology. *Phys. Rev. B* **73**: 045322.

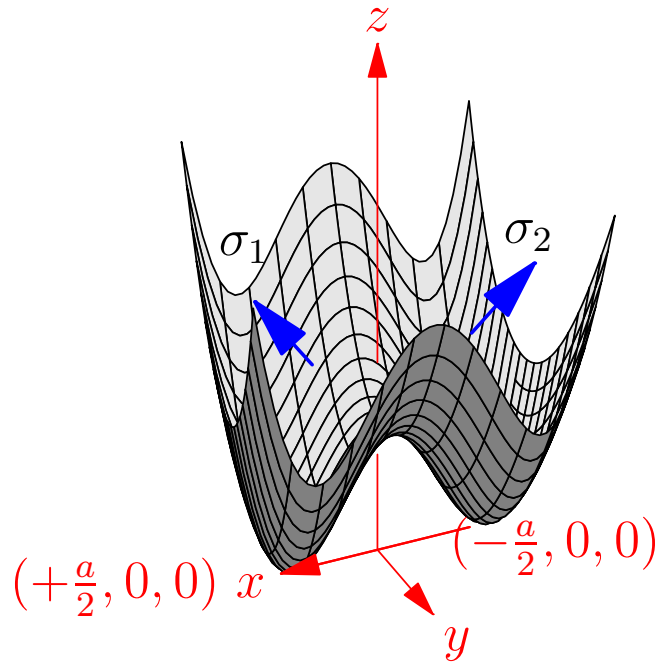


FIG. 1. Two-dot potential (3). Blue (dark grey) arrows indicate electron's spins.

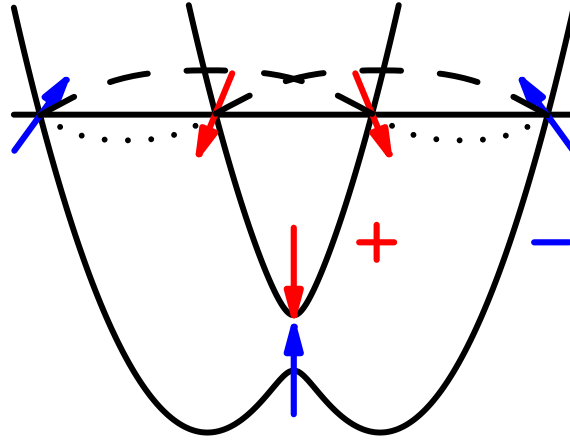


FIG. 2. Occupied subbands  $\epsilon_{\pm}$  of Eq. 24 for  $\beta = 0$ . Arrows illustrate spin polarization in different subbands. Dashed (dotted) lines indicate exchange (direct) Cooper scattering processes. Reprinted with permission from (Gangadharaiah et al. 2008a). Copyright (2008) by the American Physical Society.

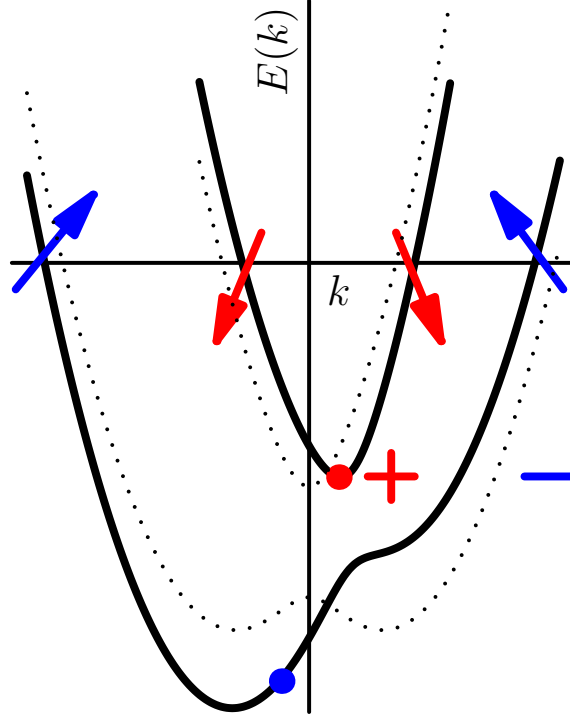


FIG. 3. Occupied subbands  $\epsilon_{\pm}$  for the case of non-orthogonal spin-orbital and magnetic field axes,  $\beta \neq 0$ . Arrows illustrate spin polarization, as in Fig. 2. Filled dots indicate location of the center-of-mass for (+) (red) and (-) (blue) subbands, which shift in opposite directions. Dashed lines show ( $\pm$ ) subbands of Fig. 2, corresponding to the orthogonal orientation,  $\beta = 0$ , for comparison. Reprinted with permission from (Gangadharaiah et al. 2008a). Copyright (2008) by the American Physical Society.

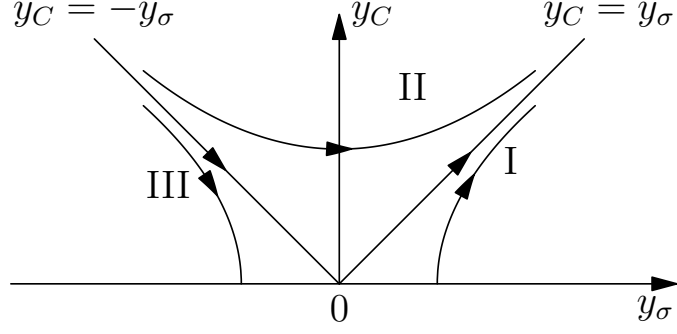


FIG. 4. RG flow of Eq.(52). Here  $y_\sigma = g_z/(2\pi v_F)$  while  $y_C = g_\perp/(2\pi v_F)$ . Initial conditions on these couplings, as derived in (51), are such that region III is *not* accessible. All possible initial values lead to strong coupling,  $y_C \sim y_\sigma \rightarrow \infty$ . Reprinted with permission from (Gangadharaiah et al. 2008a). Copyright (2008) by the American Physical Society.